# Time-Varying Robustness Margins for Wind Turbines

Sanjana Vijayshankar[1] and Peter Seiler[2]

***Abstract*— This paper focuses on robustness analysis for wind turbine control systems. The dynamics of a wind turbine are nonlinear and time-varying due to several effects including blade rotation, wind shear, tower shadowing, and varying wind conditions. Thus classical gain/phase/delay margins, computed using frequency domain concepts, are insufficient for turbine control systems. The robustness analysis in this paper is instead performed in two steps. First, the turbine dynamics are linearized at either constant wind conditions or along a fixed (hub height) wind speed trajectory. This yields a linear time-varying (LTV) model for the turbine dynamics. Next, disk margins are computed using existing results for finite-horizon LTV systems. These disk margins account for uncertainty at the blade pitch and/or generator torque inputs. This method is applied to assess the margins for a 2.5 MW Clipper Liberty turbine operated by the University of Minnesota. The turbine model and source control law used in the analysis was provided by Clipper. These results provide additional insight into the robustness of the existing turbine control law.**

## I. INTRODUCTION

This paper applies a time-varying approach for robustness analysis of wind turbines. The proposed approach is applied to assess the robustness margins for a 2.5MW Clipper Liberty turbine operated by the University of Minnesota. A wind turbine is inherently nonlinear and time varying. Aerodynamic torques and bending moments depend nonlinearly on wind speed, pitch angle, and tower and blade deflections. Further, there is variation as the rotor turns to position the blades in a turbulent wind profile that varies spatially with respect to the rotor disk even in constant wind conditions. These aspects contribute to the challenges in the control and analysis of wind turbines. Nevertheless, good results have been obtained using linear approximation of the wind turbine systems.

Control systems are designed using mathematical models that are only approximate representations of the real hardware. Since discrepancies between a system and its model representation may lead to a violation of some performance specification, or even closed-loop instability, accounting for modeling errors is necessarily an integral part of the design process. Classical gain and phase margins are widely used in analyzing the effect of model uncertainties on system stability for LTI systems. However, these metrics only use simple effects in model variation and have a frequency domain, infinite horizon argument.

This paper describes a time-domain approach to assess disk margins for a utility-scale turbine. A similar method applied to rocket launchers can be found in [1]. The method proposed here is performed by first linearizing the turbine dynamics using an aeroelastic simulator, FAST (Fatigue, Aerodynamics, Structures, and Turbulence) [2], that is capable of generating linearized models of the Clipper turbine at specific wind trim conditions and azimuth positions. Time-varying models are constructed at either constant or (fixed) time-varying wind conditions. Next, the baseline control law of the Clipper turbine is linearized. The uncertain closed-loop system is formed with symmetric disk margin type uncertainty inserted between the plant and the controller. Small gain theorem is applied to obtain a sufficient condition for robustness margins in terms of an induced $\mathcal{L}_2$ gain of a related system (Section III-B). Subsequently, existing results are used to compute the finite horizon $\mathcal{L}_2$ gain [3] of the system (Section III-A). Disk gain and phase margins are then computed using the equations described in Section III-C.

Several results are presented in this paper highlighting the advantage this approach has over the conventional LTI analysis that is performed at constant wind conditions. Firstly, robustness margins are evaluated considering uncertainty one loop at a time (Section IV-A) assuming wind speed to be constant. Next, uncertainty is considered concurrently in all the loops (Section IV-B). In each of the above cases, a comparison is done with the conventional time-invariant analyses. The final and the most important result considers the case when the wind conditions are time-varying (Section IV-C). These insights can be very useful to assess if the turbine is close to going unstable if we have a wind forecast available. Drastic wind speed changes can drive the wind turbine system to instability and this algorithm can help take corrective measures to avoid that.

## II. MODEL DESCRIPTION

### A. Clipper Turbine

Fig. 1. Clipper Liberty 2.5MW Research Turbine [4]

The turbine considered in this paper is the Clipper C96 Liberty Wind Turbine (See Figure 2). This turbine is owned and operated by the Eolos Wind Energy Research Consortium [4] at the University of Minnesota (UMN). The basic data for this turbine is given in Table I. The source code for the control law operating on this turbine was previously provided by Clipper to UMN. This industrial control law is similar to existing standard wind turbine control laws [5][6].

[1]Graduate Student, Department of Electrical Engineering, University of Minnesota, vijay092@umn.edu

[2]Associate Professor, Department of Aerospace and Engineering Mechanics, University of Minnesota, seile017@umn.edu

| Quantity | Value | Units |
|---|---|---|
| Hub Height | 80 | m |
| Rotor Diam | 96 | m |
| Rated Wind Speed | 25 | m/s |
| Rated Gen. Speed | 1133 | RPM |
| Rated Gen. Torque | 23.473 | kNm |

TABLE I
DATA FOR CLIPPER C96 LIBERTY TURBINE

The robustness analysis in this paper is performed using this industrial control law. A brief outline of the control law is provide here but full details are omitted for proprietary reasons. As is standard, the turbine control inputs include the blade pitch and generator torque. Figure 2 shows the operating regions specific to the Clipper turbine. The control law operating on the Clipper turbine is standard with a $k\omega^2$ law in Region 2 for maximum power point tracking and a PI control law to track rated rotor speed in Region 3.

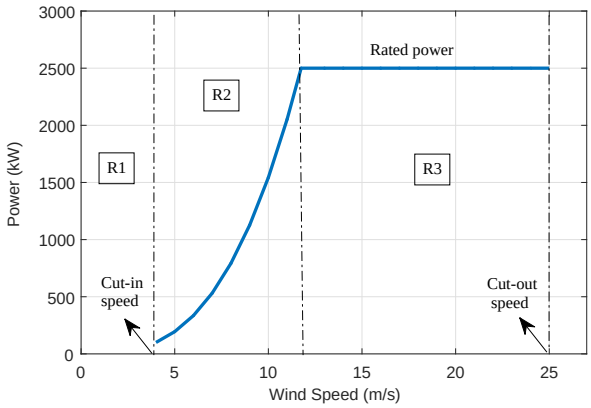

Fig. 2. Turbine Operating Regions

### B. Linearization

The dynamics of the wind turbine are nonlinear and time-varying. These dynamics are modeled using the Fatigue, Aerodynamics, Structures, and Turbulence (FAST) simulation package developed by the National Wind Technology Center [2]. A FAST model for the C96 Liberty turbine was provided to UMN by Clipper and is used for the analyses in this paper. FAST is a comprehensive aeroelastic simulation with capability to include up to 24 degrees of freedom. The analyses summarized in Section V were performed with a 17-state model that contains the generator speed, first flapwise and edgewise bending modes for each of the three blades, and first side-to-side and fore-aft tower bending modes. Including additional degrees of freedom yields a more accurate, higher fidelity model.

The analyses are performed using linearized approximations of the nonlinear wind turbine dynamics. The linearized models are constructed, using FAST, at fixed wind trim conditions of 6m/s, 7m/s, ... , 25m/s. Linear interpolation is used to obtain a linearized model at any other wind speed. Note that the turbine dynamics are time-varying, even at constant wind conditions, due to blade rotations, tower shadow, etc. Thus the linearized models returned by FAST are periodic due to their dependence on rotor angle $\phi$. Some of the analyses in Section IV will be performed using the linear time-varying (LTV) models. Alternatively, an approximate, linear time-invariant (LTI) model is obtained by using the Multi-Blade Coordinate transformation (MBC) [7] [8]. The MBC transforms quantities in the rotating frame, e.g. blade bending moments, into the fixed nacelle frame. Applying the MBC to the linearized LTV models generated by FAST yields a transformed LTV model with weak dependence on rotor angle $\phi$. Averaging the resulting state-space matrices over one rotor period yields an approximate LTI model. Note that an LTI model can only be obtained if the wind conditions are constant. This motivates the use of a time-varying model for analysis that can handle the case when the wind conditions are varying with respect to time.
The baseline control law described in Section II-A has nonlinearities. For example, the $k\omega^2$ law in Region 2 is nonlinear. Thus, the controllers are also linearized about the same trim conditions as considered in the FAST linearization. Again, these linearized models are constructed at fixed wind trim conditions 6m/s, 7m/s, ... 25m/s.

## III. TECHNICAL APPROACH

This section describes the technical approach considered for the robustness analysis of the Clipper turbine.

### A. Linear Time-Varying Systems

LTI system modeling may not describe the behavior of some systems very accurately. As a consequence, it is pertinent to make use of LTV models for some applications whose dynamics vary with respect to time. In our application, we are mainly interested in analyzing the robustness of the wind turbine when the dynamics are varying with respect to time. The main challenge is that frequency domain interpretation is not applicable to LTV systems.
Consider the following linear, time-varying (LTV) system $M$ defined on $[0, T]$:

$$\dot{x}(t) = A(t)x(t) + B(t)u(t) \tag{1}$$
$$y(t) = C(t)x(t) + D(t)u(t) \tag{2}$$

where $x \in \mathbb{R}^{n_x}$ is the state, $u \in \mathbb{R}^{n_u}$ is the input, and $y \in \mathbb{R}^{n_y}$ is the output. The state matrices $A : [0, T] \to \mathbb{R}^{n_x \times n_x}$, $B : [0, T] \to \mathbb{R}^{n_x \times n_d}$, $C : [0, T] \to \mathbb{R}^{n_e \times n_x}$, and $D : [0, T] \to \mathbb{R}^{n_e \times n_d}$ are piecewise-continuous functions of time. The state matrices are, by assumption, bounded on $[0, T]$. In addition, the analysis will be performed on a finite horizon, i.e. $T < \infty$, unless noted otherwise. As a result, $u \in \mathcal{L}_2[0, T]$ implies both $x$ and $y$ are in $\mathcal{L}_2[0, T]$ for any $x(0)$ [9].
Many different performance metrics can be defined for this (nominal) finite-horizon LTV system. This paper will use the induced gain to compute robustness metrics. Specifically, the *finite-horizon induced $\mathcal{L}_2$-gain* of $M$ is

$$\|M\|_{2,[0,T]} := \sup \left\{ \frac{\|y\|_{2,[0,T]}}{\|u\|_{2,[0,T]}} \;\middle|\; x(0) = 0, 0 \neq u \in \mathcal{L}_{2,[0,T]} \right\}.$$

As noted above, $u \in \mathcal{L}_2[0, T]$ implies $y \in \mathcal{L}_2[0, T]$. Thus the $\mathcal{L}_2$ gain is finite for any fixed horizon $T < \infty$. The next theorem provides a necessary and sufficient condition to bound the induced $\mathcal{L}_2[0, T]$ gain of $M$. This is an existing result [10], [11], [3] that will form the basis for our numerical calculations.

*Theorem 1 (Bounded Real Lemma):* Let $\gamma > 0$ be given such that $R(t) := D(t)^T D(t) - \gamma^2 I < 0$ for all $t \in [0, T]$. Then the following statements are equivalent:

1) $\|M\|_{2,[0,T]} < \gamma$
2) There exists a differentiable, function $P : [0, T] \to \mathbb{S}^{n_x}$ [1] such that $P(T) = 0$, $P(t) \geq 0$ and

$$\begin{aligned} &\dot{P} + A^T P + PA + C^T C - \\ &(PB + C^T D) R^{-1} (PB + C^T D)^T = 0 \end{aligned} \tag{3}$$

This is a Riccati Differential Equation (RDE).

### B. Small Gain Theorem

The small gain theorem [12] gives sufficient conditions under which a feedback connection of two systems is bounded-input, bounded-output stable. This section will briefly summarize the small gain theorem for the specific case of LTV systems. Consider the feedback interconnection shown in Figure 3. Let $M : \mathcal{L}_2[0, \infty) \to \mathcal{L}_2[0, \infty)$ and $\Delta : \mathcal{L}_2[0, \infty) \to \mathcal{L}_2[0, \infty)$. The feedback connection is defined by the following equations:

$$d_1 = u_1 + \Delta u_2 \tag{4}$$

$$d_2 = u_2 - M u_1 \tag{5}$$

The small gain theorem is stated next.

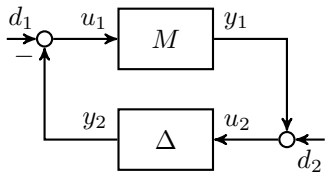


Fig. 3. Interconnection for Small Gain Theorem

*Theorem 2 (Small Gain Theorem):* Assume the feedback connection in Figure 3 is well-posed with $\|M\|_{2,[0,\infty)} < \gamma_M$ and $\|\Delta\|_{2,[0,\infty)} < \gamma_\Delta$ where $\gamma_M$, $\gamma_\Delta < \infty$. The feedback connection is bounded-input, bounded-output stable if $\gamma_M \cdot \gamma_\Delta < 1$.

Although the theorem is stated using an infinite horizon argument, it is not viable to perform our analysis on an infinite horizon. Thus, we chose a sufficiently long time horizon $[0, T]$ that is computed using the method described in Section III-D.

### C. Symmetric Disk Margins

This section briefly reviews the use of symmetric disk margins for robust stability analysis [13][14]. First recall that classical gain and phase margins account for the amount of gain or phase variation that can be tolerated by a feedback system. These margins can be interpreted in the Nyquist plane when the plant $G$ and controller $K$ are LTI. Specifically, the gain margin is the amount of gain variation that can be inserted between the plant and controller while retaining closed-loop stability. This is interpreted as an interval on the negative real axis that contains $-1$ and which excludes the Nyquist plot of $L = GK$. The phase margin is the amount of phase variation that can be tolerated while retaining closed-loop stability. This is interpreted as an arc along the unit circle that includes $-1$ and which also excludes the Nyquist plot of $L$. These margins are computed for single-input, single-output LTI feedback systems, e.g. using Bode plots.

Symmetric disk margins [15], as described further below, can be interpreted as a disk containing $-1$ that excludes $L$. There are two main reasons to use disk margins rather than classical gain/phase margins. First, it is possible (though rare) for a system to have good gain and phase margins and yet have a Nyquist plot of $L$ that comes close to -1 (i.e the feedback system is not very robust). Disk margins provide a region (in all directions) that excludes $L$. Second, symmetric disk margins can be computed from the $\mathcal{L}_2[0, T]$ norm of a specific system using the small gain theorem. This does not require a frequency response and hence generalizes naturally for LTV feedback systems. Moreover, it yields a numerical procedure to compute multi-loop margins for multi-input, multi-output systems. This is useful for assessing the robustness of the wind turbine feedback system. In particular, the multi-loop margins correspond to robustness with respect to (independent) uncertainty introduced into the blade pitch and generator torque feedback paths.

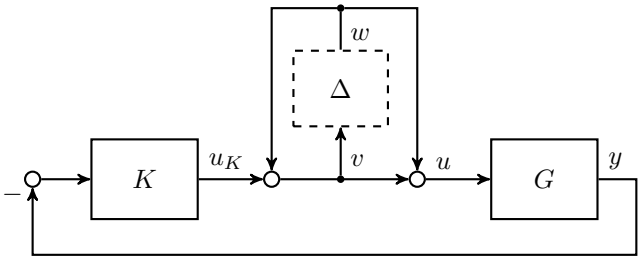


Fig. 4. Symmetric Disk Margin Setup

Symmetric disk margins are computed by introducing an LTI uncertainty $\Delta$ into the feedback loop as shown in Figure 4. The plant $G$ and/or controller $K$ can be LTV systems but are assumed, for this initial discussion to be SISO. The closed-loop system in Figure 4 can be brought into the form shown in Figure 3 with $M := (S - T)$ where $S := \frac{1}{1+KG}$ and $T := \frac{KG}{1+KG}$ are the sensitivity and complementary sensitivity at the plant input, respectively. Assume $\|M\|_{2,[0,T]} < \gamma$. By the small gain theorem, the feedback loop is stable for all $\|\Delta\| \leq \frac{1}{\gamma}$ and $\frac{1}{\gamma}$ is the symmetric disk margin. This result can be used to provided guaranteed bounds on the classical gain and phase margins. Specifically, the feedback system in Figure 4 is equivalent to the one shown in Figure 5.

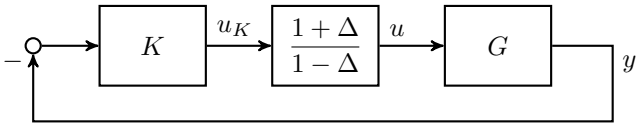


Fig. 5. Simplified Symmetric Disk Margin Interconnection

Assume $\|M\|_{2,[0,T]} < \gamma$ and denote the symmetric disk

[1] Here $\mathbb{S}$ denotes the set of symmetric matrices with the dimension given in the superscript.

margin as $r_{min} := \frac{1}{\gamma}$. It can be shown, based on Figure 5, that the feedback loop is stable for gain variations in the range $\left[\frac{1-r_{min}}{1+r_{min}}, \frac{1+r_{min}}{1-r_{min}}\right]$ [13][14][15]. The disk gain margin thus is:

$$GM_l = \frac{1 - r_{min}}{1 + r_{min}}, \quad GM_u = \frac{1 + r_{min}}{1 - r_{min}} \tag{6}$$

Similarly, an expression for the disk phase margin is:

$$\text{PM}_l = -2\cot(r_{min}), \quad \text{PM}_u = 2\cot(r_{min}) \tag{7}$$

Note that bounds on the symmetric disk margin can, via the small gain theorem, be computed for LTV systems from the induced $L_2$ gain of a related system $M$.

### D. Algorithmic Implementation

Using the results mentioned above, an algorithm is written to compute symmetric disk margins for the wind turbine system with the baseline controller. The first step in this implementation is to get the state-space matrices of the block $M$ mentioned in III-C. A linearization of the FAST turbine model is utilized to obtain the plant state matrices. The model is linearized about specific trim conditions $(\bar{\beta}, \bar{\tau}, \bar{\omega})$ where $\bar{\beta}, \bar{\tau}$ and $\bar{\omega}$ are the trim blade pitch, generator torque and rotor speed of the plant at a trim wind speed $\bar{v}$. This is done for various wind speeds ranging from $6m/s$ to $25m/s$. Also note that FAST produces state matrices at azimuth angles $(\phi)$ spread $2\,\text{deg}$ apart from $0\,\text{deg}$ to $358\,\text{deg}$. A total of 180 state matrices is obtained. If the blade bending degrees of freedom are not enabled while linearizing, the matrices will be very close to each other. However, there might be significant differences in the matrices from one azimuth angle to another i.e., the models will vary as the blades traverse from $0\,\text{deg}$ to $360\,\text{deg}$. Thus, state-matrices are obtained for various azimuth angles and wind speeds. These are integrated together to form matrices of the form $A_{cl}(\phi, v)$, $B_{cl}(\phi, v)$, $C_{cl}(\phi, v)$ and $D_{cl}(\phi, v)$ where:

$\phi$ = Azimuth angle in degrees
$v$ = Wind speed in $m/s$

With this, we have state matrices at just 180 different azimuth locations and at various wind speeds from $6m/s$ to $25m/s$. But this is not adequate for our analysis. $\phi$ and $v$ are quantities that are dependent on time. Thus, in order to obtain a time-varying model of the turbine, we need state matrices at every azimuth angle and wind speed. This is accomplished by interpolating $\phi$ and $v$ over a rectilinear 2D grid. The process is called bilinear interpolation and this dynamically gives the right state matrices as time progresses.

Given these state matrices, the induced $\mathcal{L}_2[0, T]$-norm is computed from Theorem 1. A bisection method is employed to find the $\gamma$ such that $\|M\|_{2,[0,T]} < \gamma$ until the gamma selected comes arbitrarily close to the induced $\mathcal{L}_2$-norm, $\|M\|_{2,[0,T]}$. The existence of a solution to the Riccatti Differential Equation 3 and the positive semi-definiteness of $P(t)$ is checked in every iteration of the bisection algorithm. The disk margins of the closed-loop system are then calculated using the procedure described in III-C.

The time-horizon, for the purpose of this analysis, has been approximately chosen based on the settling time of the equivalent LTI model because running computations over an infinite horizon is infeasible. For this wind turbine system, it is observed that at constant wind conditions, the settling time is higher for higher wind speeds. Exploiting this fact, we find the peak wind speed in the wind speed data given. For instance, consider the wind profile shown in Figure 9. The peak wind speed here is $22.8m/s$. We then find the settling time $(t_s)$ of the system using its step response. Next, we validate this against the final time $(t_f)$ in the wind speed data given. If $t_f \geq t_s$, then the time horizon is sufficiently long and can be used for our analysis. If not, we can get data spread over a longer horizon and then proceed. In this case, $t_f = 25s$ and $t_s = 20s$. Thus, we can make an infinite horizon approximation for this time-varying system.

## IV. RESULTS AND DISCUSSION

This section explains the robustness analysis of the Liberty wind turbine that incorporates the baseline control architecture described in Section II-A. Since multiple SISO loops are involved in this setup, there are many forms of uncertainties that can be considered. Results pertaining to three different forms of uncertainties have been presented below. The control inputs, blade pitch and generator torque are controlled by two different control laws. The effect of uncertainty is considered loop-at-a-time first and then considered simultaneously in both the channels. Furthermore, a time-varying analysis of the turbine is presented when the wind speed follows a prescribed (not necessarily constant) trajectory varying in time.

### A. Loop-at-a-time Analysis

The closed-loop model of the Clipper turbine with the baseline control architecture consists of 2 SISO loops. Loop-at-a-time margins analyze the effect of uncertainty in one channel on the entire system. The plant model considered in this analysis is described in Section II-B. The analysis is performed for fixed wind speeds from $6m/s$ to $25m/s$. As noted previously, the linearized turbine models are time-varying even when wind speeds are fixed due to the rotational effect. Thus, the state matrices described in III-D get simplified to $A_{cl}(\phi)$, $B_{cl}(\phi)$, $C_{cl}(\phi)$ and $D_{cl}(\phi)$. Since the feedback loop mainly consists of two SISO loops, two types of uncertainties have been considered in this section. Symmetric disk margin uncertainty is injected in the blade pitch or generator torque loops individually. Induced $\mathcal{L}_2[0, T]$-gain and symmetric disk margins are then calculated using the procedure described in Section III.

First, the analysis is performed using a 1-state model of the turbine which only includes the generator degree-of-freedom. Next, it is performed using the 17-state model described in Section II-B. Figures 6 and 7 show the lower bounds $(GM_l)$ on the LTV disk margins as a function of wind speed for both the torque (blue diamond) and pitch uncertainty (red circle). Due to the symmetric nature of the margins, the upper-bound is simply $GM_u = 1/GM_l$. The torque loop is only active in regions 2 and 2.5. As a result, the symmetric disk margins are $[0, \infty)$ (the closed-loop is all-pass with unity gain) and are not shown for Region 3. Similarly, the pitch loop is active only in regions 2.5 and 3. Hence the symmetric disk margins for the blade pitch are not shown in Region 2.

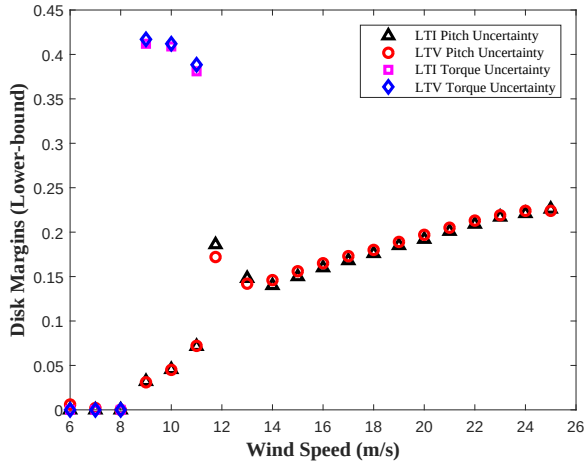


Fig. 6. Disk gain margin lower bounds (1-state model) with uncertainty considered one loop at a time.

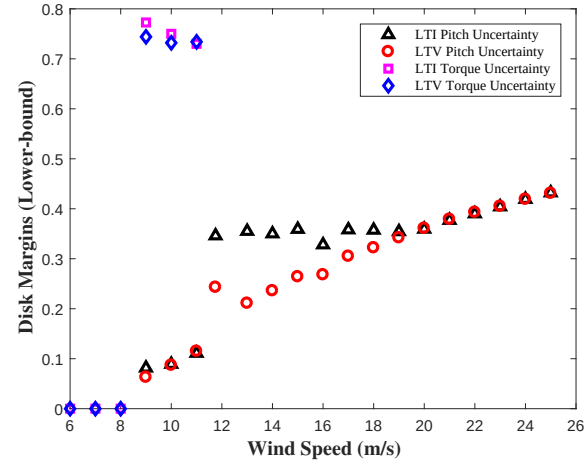


Fig. 7. Disk gain margin lower bounds (17-state model) with uncertainty considered one loop at a time.

When wind speeds are fixed, MBC transformation and averaging, explained in Section II-B, can be used to obtain an approximate LTI model. Figure 7 shows bounds on the LTI disk margins as a function of airspeed for both the LTI torque (magenta square) and LTI pitch uncertainty (black triangle).

It can be seen that when the rotating degrees of freedom are not included, i.e., in the 1-state model case (Figure 6), the LTI and LTV disk margins exactly line up. However, there are differences in the LTI/LTV disk margins for the 17-state model case (Figure 7). Specifically, the margins deviate from each other from 12m/s to 18m/s. Although these differences can be attributed to the rotating degrees of freedom and the approximation technique used to obtain the time-invariant model, it is unclear, however, why these differences exist only in the wind speed range $12m/s - 18m/s$. We hypothesize that the collective degree-of-freedom obtained using MBC transformation matches the three out-of-plane degrees of freedom of the individual blades at higher wind speeds. Additionally, the 17-state model has significantly higher lower-bounds than the 1-state model indicating that system may not be as robust as it seems in the 1-state model.

### *B. Multi-loop Analysis*

In this section, we discuss the case when there is uncertainty in both the pitch and torque feedback loops. These are allowed to vary simultaneously. Since the uncertainty block here is multi-input multi-output, there are different forms of structures that can be considered. In our analysis, we are mainly interested in analyzing uncertainty that is decoupled in nature. This analysis describes how much independent and concurrent symmetric disk variation can occur independently in each feedback channel while maintaining stability of the closed-loop system. Thus, the structure of the uncertainty block for $\Delta_1$,$\Delta_2 \subset \mathbb{C}$ boils down to:

$$\Delta = \begin{bmatrix} \Delta_1 & 0 \\ 0 & \Delta_2 \end{bmatrix} \tag{8}$$

Figure 8 shows both the LTV disk margins (lower) bounds as a function of wind speed with the uncertainty introduced in both the blade pitch and generator torque loops. As noted in Section II-B, the MBC transformation and averaging can be used to obtain an approximate LTI model at fixed wind speeds. Figure 8 also shows disk margin (lower) bounds for these LTI models. The multi-loop margins result in a structured uncertainty as shown in Equation 8. Hence constant D-scales can be used to reduce the conservatism in the induced $\mathcal{L}_2[0,T]$-gain condition that appears in the small gain theorem. This is similar to the use of D-scales in structured singular value analysis [16][17][18]. The LTV results were obtained with a D-scale of the form:

$$D = \begin{bmatrix} d & 0 \\ 0 & 1 \end{bmatrix} \tag{9}$$

where $d > 0$. This involves a solution to a convex optimization problem. Since the objective is non-differentiable, an approximate gradient descent algorithm with constant step size is implemented to solve the problem.

Note that the generator torque alone is active in Region 2

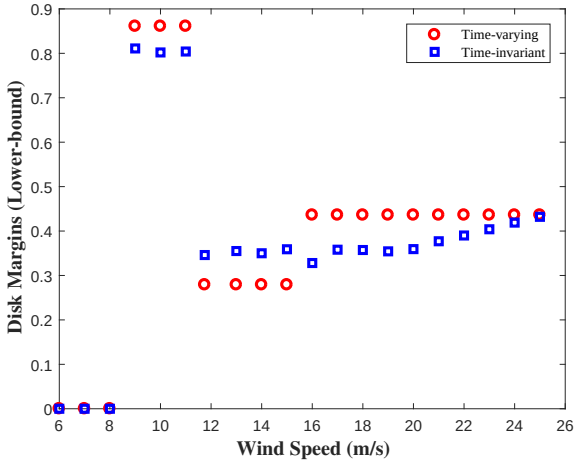


Fig. 8. Disk Margin lower bounds (17-state model) with multi-loop uncertainty

and hence the blade pitch uncertainty has no effect at low wind speeds. Thus, the results in Figures 7 and 8 are similar in Region 2. Similarly, the only loop active in Region 3 is the blade pitch feedback loop and hence the generator

torque uncertainty has no effect at high wind speeds. Thus, the results in Figures 7 and 8 are similar in Region 3. However, since both the torque and pitch loops are active in Region 2.5, it is useful to analyze the the effect of multi-loop uncertainty. In this region, the uncertainty in the two loops can interact. It can be seen that the turbine has much smaller stability margins (between 0.8 and 0.9) in Region 2.5 (9-11.75m/s). This indicates a potential robustness issue due to the interacting uncertainty in the two loops. Finally, note that the LTI/LTV results are similar again indicating that the rotational time-varying effects are minor at fixed wind speeds.

### C. Variable Wind Conditions

Results discussed till now were focused on frozen wind conditions. The main advantage of the algorithm is its ability to handle varying wind conditions. Section III-D explains how the proposed algorithm is modified so that the input to the algorithm is a varying wind speed profile and the output is the disk gain margin. Several wind speed profiles can be considered in this case but that which is of most interest to us is the behavior of the turbine at high wind speeds. Wind gusts at high mean wind speeds are typically used to examine the effect of structural loads on the turbines. An extreme and canonical example is the so-called "Mexican-hat" gust shape, as it is presented in Figure 9. Its sudden change in wind shape can possibly cause extreme changes in load or even closed-loop instability. Simulations are performed to verify this claim. Both loop-at-a-time and multi-loop analyses are carried out for this wind gust profile.

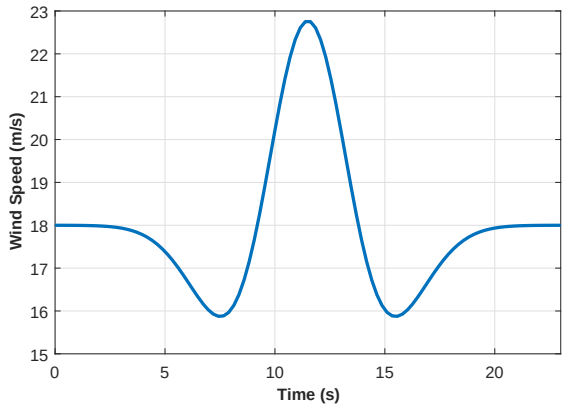


Fig. 9. Mexican Hat Wind Gust

First, the uncertainty is considered in the torque loop. Since, the torque loop is inactive in Region 3, which is where the turbine is operating for the given wind gust, the disk gain margins are $[0,\infty)$. In other words, the finite-horizon induced $\mathcal{L}_2$-gain is $\approx 1$. Second, uncertainty is considered in the pitch loop and the resulting disk gain margin is $[0.436, 2.293]$. It also follows, due to the fact that there is only one active feedback loop, that the multi-loop margins are same as that of loop-at-a-time margins considered in the pitch feedback path i.e., $[0.436, 2.293]$.

The results indicate a reduction in the robustness margins of the turbine as compared to the ones obtained at frozen wind conditions. This shows that frozen wind speed analysis is insufficient to conclude anything about the robustness of the system and also necessitates a rigorous time-varying analysis to gain better insights into the robustness of the system.

## V. CONCLUSIONS

This paper applies a time-varying approach for robustness analysis of the 2.5 MW Clipper Liberty turbine. A time-varying model is first constructed by linear interpolation of LTI models at different wind trim conditions obtained from FAST. The state matrices are then utilized to compute the finite-horizon induced $\mathcal{L}_2[0,T]$-gain. Small Gain Theorem is then used to compute disk gain margins of the system. Loop-at-a-time and multi-loop analysis is performed for both frozen and varying wind conditions. This approach can be very useful in analyzing the robustness of the turbine given real wind speed data from the turbine. Future research could explore better control techniques if the margins are found to be too low.

## ACKNOWLEDGMENT

This work was supported by the National Science Foundation under Grant No. NSF-CMMI-1254129 entitled CAREER: Probabilistic Tools for High Reliability Monitoring and Control of Wind Farms.

## REFERENCES

[1] F. Biertuempfel and H. Pfifer, "Worst case gain computation of linear time-varying systems over a finite horizon," submitted to 2nd IEEE Conference on Control Technology and Applications, 2018.
[2] J. M. Jonkman and M. L. Buhl Jr, "FAST user's guide-updated august 2005," tech. rep., National Renewable Energy Laboratory (NREL), Golden, CO., 2005.
[3] M. Green and D. J. N. Limebeer, *Linear Robust Control*. Prentice Hall, 1995.
[4] Eolos, "Eolos wind energy research consortium." Online; accessed 3 September 2017.
[5] T. Burton, N. Jenkins, D. Sharpe, and E. Bossanyi, *Wind energy handbook*. John Wiley & Sons, 2011.
[6] E. Bossanyi, "Developments in closed loop controller design for wind turbines," in *ASME Wind Energy Conference*, p. 64–74, 2000.
[7] G. S. Bir, "Multi-blade coordinate transformation utility for 3-bladed wind turbines," tech. rep., Technical report, NREL, 2008.
[8] G. Bir, "Multiblade coordinate transformation and its application to wind turbine analysis," in *ASME Wind Energy Symposium*, pp. 1–15, 2008.
[9] R. Brockett, *Finite Dimensional Linear Systems*. SIAM Classics in Applied Mathematics, 2015.
[10] G. Tadmor, "Worst-case design in the time domain: The maximum principle and the standard $H_\infty$ problem," *Mathematics of Control, Signals, and Systems*, vol. 3, pp. 301–324, 1990.
[11] R. Ravi, K. Nagpal, and P. Khargonekar, "$H_\infty$ control of linear time-varying systems: A state-space approach," *SIAM Journal of Control and Optimization*, vol. 29, no. 6, pp. 1394–1413, 1991.
[12] C. A. Desoer and M. Vidyasagar, *Feedback systems: input-output properties*. New York: Academic Press, 1975.
[13] D. Bates and I. Postlethwaite, *Robust multivariable control of aerospace systems*, vol. 8. IOS Press, 2002.
[14] J. D. Blight, R. Lane Dailey, and D. Gangsaas, "Practical control law design for aircraft using multivariable techniques," *International Journal of Control*, vol. 59, no. 1, pp. 93–137, 1994.
[15] M. F. Barrett, "Conservatism with robustness tests for linear feedback control systems," in *Decision and Control including the Symposium on Adaptive Processes, 1980 19th IEEE Conference on*, vol. 19, pp. 885–890, IEEE, 1980.
[16] S. Skogestad and I. Postlethwaite, *Multivariable feedback control: analysis and design*, vol. 2. Wiley New York, 2007.
[17] A. Packard and J. Doyle, "The complex structured singular value," *Automatica*, vol. 29, no. 1, pp. 71–109, 1993.
[18] A. Packard, M. K. Fan, and J. Doyle, "A power method for the structured singular value," in *Decision and Control, 1988., Proceedings of the 27th IEEE Conference on*, pp. 2132–2137, IEEE, 1988.